Thermodynamic Consistency between Analytic Integral Equation Theory and Coarse-Grained Molecular Dynamics Simulations of Homopolymer Melts

DATASET *in* MACROMOLECULES · NOVEMBER 2012

Impact Factor: 5.8 · DOI: 10.1021/ma301502w

4 AUTHORS:

James Mccarty
ETH Zurich
14 PUBLICATIONS **110** CITATIONS
SEE PROFILE

Anthony Clark
Columbia University
11 PUBLICATIONS **85** CITATIONS
SEE PROFILE

Ivan Lyubimov
University of Chicago
19 PUBLICATIONS **143** CITATIONS
SEE PROFILE

Marina Guenza
University of Oregon
89 PUBLICATIONS **908** CITATIONS
SEE PROFILE

Macromolecules

Article

pubs.acs.org/Macromolecules

Thermodynamic Consistency between Analytic Integral Equation Theory and Coarse-Grained Molecular Dynamics Simulations of Homopolymer Melts

J. McCarty,[†] A. J. Clark,[†] I. Y. Lyubimov,[†] and M. G. Guenza*[,†,‡]

[†]Department of Chemistry and Institute of Theoretical Science, University of Oregon, Eugene, Oregon 97403, United States

[‡]Kavli Institute for Theoretical Physics, University of California, Santa Barbara, California 93106-4030, United States

ABSTRACT: We present the equation of state for a coarse-grained model of polymer melts where each chain is represented as a soft colloidal particle centered on its center-of-mass. The formalism is based on the solution of the Ornstein−Zernike equation and is analytical, allowing for the formal investigation of the elements that ensure thermodynamic consistency in coarse-grained models of polymer melts. By comparing predictions from our expressions with those from computer simulations of the coarse-grained system and with atomistic polymer integral equation theory, we demonstrate that both structural and thermodynamic consistency with the atomistic level description is maintained during our coarse-graining procedures.

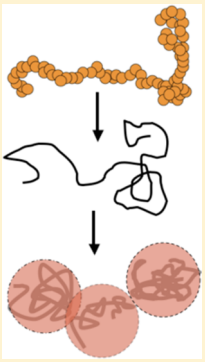

1. INTRODUCTION

Coarse-graining (CG) models are receiving widespread attention, being the necessary tools that allow one to simulate complex systems, where phenomena develop on a wide range of length scales from the atomistic to the macroscopic description. CG models are derived by averaging out local degrees of freedom at a length scale shorter than a characteristic length, and obtaining in this way a new description in the coordinates of the resulting CG units, where the system interacts through an effective potential. The new CG description has the advantage that the length and time scale of the elementary step in the CG simulation are increased, the CG simulation accelerated, and the maxium length and time scales that the CG simulation can cover significantly extended. To be valid, the coarse-graining description has to predict correctly and consistently the system structural and thermodynamic properties at length scales larger than the characteristic CG length.

Coarse-grained models (CG) have become particularly prevalent for studying polymer liquids, as these systems are characterized by a broad range of coexisting time and length scales.[1,2] Although computer simulations can provide a wealth of information about the physics of condensed matter systems of small size, for polymeric materials it is necessary to perform simulations of increasingly long chains, i.e., increasing degree of polymerization, N, and increasingly large box sizes, because qualitative differences in chain dynamics and large-scale liquid structure for macromolecular mixtures emerge as the degree of polymerization increases. These large-scale properties are important for many applications in the engineering of novel materials. However, long polymer chains are difficult to equilibrate from a random initial configuration using conventional techniques,[3] and the computational time of the simulation run is also increased as a function of N with an exponent larger than linear, due to the large number of pairwise interactions that must be calculated at each time step of the simulation.[4,5]

Coarse-graining is a natural route for macromolecular systems, since the computational cost and equilibration times may be reduced by simplifying the underlying atomistic details in a lower-resolution model. Nonetheless, since the local chemical environment in a polymer system induces an interdependence between features on different scales, the accuracy behind a coarse-graining procedure will rest on its ability to account for monomeric information and must remain system specific. Notwithstanding the fact that macroscopic properties depend on the specific monomeric picture, it is not a trivial matter to formally connect through a theoretical approach large properties with local scale structure of the macromolecular liquid. In this perspective, a theoretically sound coarse-grained description of macromolecular systems, obtained from the first-principle solution of fundamental equations for the structure of polymer liquids, and which is shown to correctly reproduce not only the structural but also the thermodynamic properties of the real macromolecular system, is a highly desirable goal. Such a model would have the potential for becoming a powerful tool for understanding

Received: July 18, 2012
Revised: September 12, 2012
Published: October 9, 2012

synthetic polymeric materials in the regions of phase space that are not reachable by simple atomistic simulations.

In a series of recent papers, we have developed a liquid state theory for the coarse-graining of polymer melts, block copolymers, and polymer mixtures, where chains are represented as soft spheres[6−8] or chains of soft blobs.[9,10] In this paper, we derive the analytical equation of state for the simplest of these systems, a homopolymer melt represented as a liquid of soft spheres, starting from our first-principles coarse-graining procedure and a new analytic formulation of the effective potential. Thermodynamic consistency is maintained in our approach during coarse-graining and the comparison of predictions from our expressions with those from computer simulation and with polymer integral equation theory shows full consistency.

While coarse-graining invariably aims at reducing the complexity of the underlying system, it is nonetheless important that a mesoscopic description correctly reproduces thermodynamic properties of the real system. Many coarse-graining methods have been developed in recent years[11−16] with a vast majority of them being numerical, meaning that the effective pair potential is numerically optimized to reproduce some particular property calculated from a more detailed-level simulation. For example, a widely used procedure is the Iterative Boltzmann Inversion (IBI) technique,[17] where an initial guess of the effective potential, $v_0(r)$, usually taken as the potential of mean force $[v_0(r) = -k_BT \ln g(r)]$ is used in a trial simulation, yielding a new radial distribution function, $g_0(r)$, which is different from the target $g(r)$. This provides a correction term to the pair potential by Boltzmann inversion of the difference in the radial distribution functions, $k_BT \ln[g_0(r)/g(r)]$. This procedure is then iterated until the effective pair potential reproduces the correct target radial distribution function (RDF) as measured in an atomistic simulation. Examples of other structure-based approaches include the inverse Monte Carlo method,[18] the multiscale coarse-graining (MS-CG) approach, which is based on a force-matching procedure,[19,20] and the structure-based method of Kremer and co-workers.[15,21] Another approach of Nielsen, et al. optimizes coarse-grained potentials to match experimental bulk density and surface tension values,[22] while a coarse-grained model for DNA has been proposed for which the force field parameters are obtained through an iterative procedure to match experimental melting temperatures.[23,24]

The abundance of coarse-graining procedures in the literature have revealed two deep-seated problems inherent to any numerical optimization scheme. Following the argument outlined by Louis,[25] the first is a problem of *transferability*, namely, that an effective pair potential optimized at one set of thermodynamic conditions will not generally be transferable to another set of conditions. This is a consequence of coarse-graining, as the effective potential is a free energy of the system, and thus is state-dependent. In principle, the pair potential optimized at one density, temperature, and composition is not the same as that optimized at any other density, temperature, and composition, and one would need to optimize a new effective potential for each thermodynamic state of the system, which defeats the overall purpose of coarse-graining since the potential must be optimized to match an atomistic-level simulation. Typically, as the explicit state-dependence is unknown, a numerically optimized pair potential will have a limited range of applicability to a subset of states close to the one at which the potential was derived.[26,27] This feature limits the applicability of coarse-grained potentials for studying systems at conditions far from those of conventional simulations, such as systems approaching the glass transition.

The second problem for numerical coarse-graining methods is a problem of *representability*. It has been theoretically shown by Henderson that any isotropic potential which reproduces the correct pair structure of a fluid is unique up to a constant.[28] Consequently, for any given structure, there is one unique effective pair potential which will reproduce the correct radial distribution function, and in principle any thermodynamic property of interest, since knowledge of the structure (along with the proper closures for integral equations), completely specifies the thermodynamic state of the system.[29,30] However, even at the correct state conditions, numerical potentials optimized to reproduce one quantity (for example, the correct RDF), will not necessarily reproduce any other, such as the correct pressure or internal energy. Consequently, one obtains a different effective potential depending on the property against which the coarse-grained system was optimized. For example, Johnson et al. found that coarse-grained potentials for water, optimized to reproduce the correct radial distribution function, do not reproduce the correct average internal energy or virial pressure.[31]

There are at least two reasons why numerical coarse-grained potentials fail to resolve thermodynamic properties even though they may produce the apparent correct structure. The first problem is due to an imperfect representation of the target RDF, which will introduce errors into the effective potential due to the optimization scheme. This problem is particularly difficult to avoid in numerical optimization methods, since the procedure depends on an atomistic simulation, which always introduces some error into the calculation. This is important as it has been observed that visibly different potentials may produce structures with near identical radial distribution functions to within line thickness.[32] On the other hand, many thermodynamic properties depend sensitively on the form of the interaction potential. Thus, although small errors introduced into the numerical optimization procedure do not appear to be important in determining the correct radial distribution function, they become important in the calculation of other thermodynamics properties.[33] As a result, it is often necessary to postoptimize the system to obtain the correct thermodynamics after structural optimization is complete.[16]

A second reason for the representability problem stems from the fact that, during coarse-graining, many microscopic degrees of freedom are averaged out, resulting in a simplified energy landscape and different entropy. Because it is not possible to know how a specific numerical coarse-grained potential depends on its state parameters, it is not clear how to make corrections when one expects the two levels of description to be different, for example in terms of the entropy of the system.[35]

Our model follows an alternative, formally sound, coarse-graining method which is analytical as opposed to the numerical schemes mentioned above.[6−8] The formalism rigorously maps an ensemble of polymer chains onto a system of interacting *soft* colloidal particles. Each chain is represented as a soft sphere positioned about the center of mass with a long-ranged repulsive interaction of length scale on the order of the polymer radius of gyration and a small attractive component that stabilizes the liquid.

Having an analytical solution is desirable for several reasons. Importantly, the state-dependence of the effective potential is

explicitly known, and thus the transferability problem is solved outright. Second, having an analytical solution avoids the need to optimize the effective potential against a more detailed description, hence avoiding the inclusion of numerical errors arising from the atomistic simulation. Finally, having an analytical formula essentially solves the representability problem, since any thermodynamic quantity can be calculated analytically. The resulting expression can then be compared to a more detailed model and the correction terms can be directly identified if the two levels of description differ. For, example, we have recently developed such a procedure to reconstruct the "real" friction and entropy from a coarse-grained simulation to reproduce the correct center of mass displacement as measured in experiments and atomistic simulations.[36]

Although analytical models have clear advantages over numerical ones, including, for example, the fact that in principle it is not necessary to run atomistic simulations to parametrize the potential at each thermodynamic condition, it is important to notice that some systems do not allow for an analytical solution of the coarse-grained potential and numerical optimizations are the only possible approach to the problem. This is the case, for example, when the coarse-grained unit includes a limited number of atoms, and the statistics is not Gaussian. For this small level of coarse-graining the possible error in a numerical optimization of the potential is contained, but the gain in computer time due to coarse-graining is also limited. In this way, numerical and analytical coarse-graining methods are complementary tools that apply to the same system but on different levels of coarse-graining.

In this paper we derive and discuss the thermodynamic properties of our coarse-grained model, including the equation of state, for the soft-colloidal description of the polymeric liquid. The following section provides the theoretical background about our coarse-graining procedure, which is based on the Ornstein–Zernike equation for polymeric liquids where coarse-grained units are described as auxiliary sites and the monomeric units are real sites. This section also briefly describes the analytical forms of the direct correlation function and of the effective potential between coarse-grained units, which are used in the calculation of the thermodynamics for the CG system. The thermodynamic properties for the coarse-grained description are derived for a simple thread polymer model in section 3, where the equation of state in both the virial and the compressibility routes are presented. The equivalence of the thermodynamic properties derived for the CG model with the ones for the atomistic model is discussed in section 4, and comparison to simulations are presented in section 5. A brief summary concludes the paper.

2. THEORETICAL BACKGROUND: COARSE-GRAINED MODEL AND EFFECTIVE PAIR POTENTIAL

We consider a homopolymer fluid of n chains and molecular number density, ρ_{ch}, where each chain consists of N sites, or monomeric units. This description is consistent with an united atom simulation model, where each site is taken to be a CH_x group with $x = 1$, 2, or 3, or with a theoretical representation of the polymeric chain as a bead–spring model or as a thread model (see below). The overall size of the macromolecule is defined by the chain radius of gyration, R_g, which also defines the segmental size, $\sigma = (6/N)^{1/2}R_g$. This level of description we term the monomer level of description throughout this work.

At the monomer level of description, pair correlation functions are related through the polymer reference inter site model (PRISM) site-averaged Ornstein–Zernike equation[37]

$$\hat{h}^{mm}(k) = \hat{\omega}^{mm}(k)\hat{c}^{mm}(k)[\hat{\omega}^{mm}(k) + \rho\hat{h}^{mm}(k)] \tag{1}$$

where the superscript denotes monomer–monomer (mm) interactions. Here $h^{mm}(k)$ is the Fourier transform of the total correlation function, $h^{mm}(r) = g^{mm}(r) - 1$, $c^{mm}(k)$ is the direct correlation function, $\omega^{mm}(k)$ is the intrachain structure factor, and ρ is the monomer site density, given as $\rho = N\rho_{ch}$. A convenient model of the monomer structure for our purposes here, is the PRISM thread model, which treats each polymer chain as an infinite thread of vanishing thickness, such that the monomer hard core diameter, $d \to 0$, and the segment number density $\rho \to \infty$, while the quantity ρd^3 remains finite. Under these simplifying conditions, the direct correlation function becomes a Dirac-delta function in real space such that, $\hat{c}^{mm}(k) = c_0$, and $c^{mm}(\mathbf{r}) = c_0\delta(\mathbf{r})$. The solution of eq 1, subject to the constraints that $g^{mm}(r \to 0) = 0$, yields the monomer pair distribution function,

$$g^{mm}_{thread}(r) = 1 + \frac{3}{\pi\rho\sigma^2 r}[e^{-r/\xi_\rho} - e^{-r/\xi_c}] \tag{2}$$

where ξ_ρ is the length scale of density fluctuations defined as $\xi_\rho^{-1} = \xi_c^{-1} + 2\pi\rho_{ch}R_g^2$, and $\xi_c = R_g/\sqrt{2}$ is the length scale of the correlation hole.[38] The direct correlation strength parameter, c_0, in the thread model is given by[39,40]

$$c_{0,thread} = -\frac{\pi\sigma^3}{3\sqrt{3N}} - \frac{\pi^2\rho\sigma^6}{108} \tag{3}$$

The thread model, which is the model adopted in field theories, has been shown to capture correctly several key features of the large-scale liquid structure, and to do so consistently both at the monomer and at the coarse-grained levels of soft-sphere and multiblobs. The thread model is adopted here for analytical convenience, as it allows for the direct comparison of the formal expressions derived at the monomer and CG levels. Although simple, the model nonetheless represents many key features of the behavior of real chains in the scaling limit of $N \to \infty$.

We now turn to our *coarse-grained description* of the polymer melt. This description we term a mesoscale description since it represents a fluid with resolution somewhere in between a fully atomistic model and a continuum model. We begin by solving a generalized Ornstein–Zernike matrix equation, similar to eq 1, treating the chain center of mass as an auxiliary site and atomic sites as real interaction sites. The solution for $h^{cc}(k)$, which is the center of mass pair correlation function, is given by Krakoviack, et al.,[41] and reads

$$\hat{h}^{cc}(k) = \left[\frac{\hat{\omega}^{cm}(k)}{\hat{\omega}^{mm}(k)}\right]^2 \hat{h}^{mm}(k) \tag{4}$$

where the $\omega(k)$'s are the intramolecular form factors, and the superscripts denote distributions between monomers (mm), between center of mass sites (cc), and between monomers with the center of mass (cm). Equation 4 bridges in a reversible and physically sound manner information from the local monomer level to the mesoscopic level, which is important in any coarse-graining formalism since many large-scale properties of a polymer system (such as viscosity, diffusion, response to shear strain, and other relaxation processes) depend on the local

dx.doi.org/10.1021/ma301502w | Macromolecules 2012, 45, 8482–8493

chemical architecture. By assuming Gaussian chain distributions for the intramolecular form factors, which is a reasonable approximation for polymer melts, Yatsenko, et al.[6] derived an analytical expression for the total distribution function between center of mass sites, $h^{cc}(k)$. For chains of $N \geq 30$, the resulting pair distribution function in real space between polymer center of masses can be approximated as[8]

$$g^{cc}_{thread}(r) \approx 1 - \frac{39}{16}\sqrt{\frac{3}{\pi}}\frac{\xi_\rho}{R_g}\left(1 + \sqrt{2}\frac{\xi_\rho}{R_g}\right)\left[1 - \frac{9r^2}{26{R_g}^2}\right] e^{-3r^2/4{R_g}^2} \quad (5)$$

Equation 5 has been shown to quantitatively describe the structure of the polymer melt on length scales of the order of R_g and larger, as compared with both atomistic and coarse grained simulations.[6,8] Furthermore, when combined with local monomer information in a multiscale modeling procedure, we are able to determine the total structure of the polymer melt on all length scales of interest.[42,43]

Evaluation of thermodynamic properties requires knowledge of the bare intermolecular pair potential between coarse-grained units. In the context of integral equation theory, the determination of the effective pair potential, $v^{cc}(r)$, inevitably involves some level of approximation that materializes in the closure used to establish the connection between $v^{cc}(r)$ and $g^{cc}(r)$.[44] In our mesoscopic treatment of homopolymer melts, use is made of the hypernetted-chain (HNC) closure

$$\frac{v^{cc}(r)}{k_BT} = -\ln[g^{cc}(r)] + h^{cc}(r) - c^{cc}(r) \quad (6)$$

since it is known to be reasonably accurate for long-range, soft-core potentials.[29] In the limit of long molecules, where the center-of-mass liquid structure is random at short length scales because chain interpenetration becomes favorable, $h^{cc}(r) \to 0$ and $\beta w^{cc}(r) \approx -h^{cc}(r)$. This latter limit is formally obtained by linearizing the contribution with respect to $\beta w^{cc}(r)$, yielding in turn $\beta v^{cc}(r) \approx -c^{cc}(r)$, which has the form of the well-known mean spherical approximation (MSA),[29,44] originally extended to treat soft cores by Rosenfeld and Ashcroft.[45] The MSA approximation has been implemented by Tang and co-workers in deriving analytical expressions for liquids interacting through a Lennard-Jones-type potential.[46] Also, in the context of PRISM integral equation theory, Schweizer and Yethiraj, have developed a reference MSA approach which is qualitatively consistent with the observed scaling of the critical temperature with chain length in phase separating fluids.[47]

To derive analytical expressions for thermodynamic quantities of interest for polymer melts in the framework of our coarse-graining model, we start from the Ornstein−Zernike equation. Given that the polymers are described as a simple liquid of soft colloids, the direct correlation function in reciprocal space, $c^{cc}(k)$, reads

$$\hat{c}^{cc}(k) = \frac{\hat{h}^{cc}(k)}{\hat{S}^{cc}(k)} \quad (7)$$

where $\hat{S}^{cc}(k) = 1 + \rho_{ch}\,\hat{h}^{cc}(k)$ is the center of mass static structure factor.[6] The effective pair potential may be obtained with substitution of eq 5 and eq 7 into the HNC closure, eq 6. In our previous papers the potential was solved numerically, and used as an input into classical molecular dynamic simulations of soft interacting spheres. Those mesoscale simulations (MS) produced center-of-mass pair distribution functions in agreement not only with the center of mass pair distribution analytical expressions, but also with the $g^{cc}(r)$ calculated directly from united atom simulations of the same polymer system, further validating the proposed procedure.[8,12] Because they reproduce the polymer structure at intermediate to large length-scales those simulations we term mesoscale simulations.

Although eq 6 can be solved numerically from $g^{cc}(r)$, an explicit analytical form of the potential is desirable as it facilitates the evaluation of thermodynamic quantities of interest. For this we use an analytical approximation for the direct correlation function in the limit of high degree of polymerization and high monomer density which we have recently derived.[33] The analytical form of $v(r)$ is obtained in the framework of the discussed approximations starting from the definition of the total correlation function

$$\hat{h}^{cc}(k) = \frac{c_0[\hat{\omega}^{cm}(k)]^2}{1 - \rho c_0 \hat{\omega}^{mm}(k)} \quad (8)$$

Substitution of eq 8 into the expression for the inverse static structure factor, given for soft colloids as $[S^{cc}(k)]^{-1} = 1/[1 + \rho_{ch}h^{cc}(k)]$, leads to an analytical expression for $[S^{cc}(k)]^{-1}$, which can be rewritten in the form

$$[\hat{S}^{cc}(k)]^{-1} = \Gamma\left[\frac{1/\Gamma + \hat{\Omega}^{mm}(k)}{1 + \Gamma\hat{\Omega}^{mm}(k) - \Gamma[\hat{\Omega}^{cm}(k)]^2}\right] \quad (9)$$

where the parameter $\Gamma \equiv -Nc_0\rho$ and the $\hat{\Omega}(k)s$ are the intramolecular form factors normalized by N, ($\hat{\Omega}(k) = \hat{\omega}(k)/N$).

We represent the intramolecular distribution functions as following a Gaussian form, which is an approximation correct for $N > 30$ in a melt, and by expanding the difference, $\hat{\omega}^{mm}(k)/N - [\hat{\omega}^{cm}(k)/N]^2$, in a Taylor series about $k = 0$. To leading order, the effective potential in real space is for $r > R_g$

$$v^{cc}_{(0)}(r) \approx k_BT\frac{45}{(5^{1/4})8\pi}\sqrt{\frac{2}{3}}\frac{\Gamma^{1/4}}{\rho_{ch}R_g^3}\frac{\sin(Qr)}{Qr}e^{-Qr} \quad (10)$$

where the numerical factor $Q = 5^{1/4}(3/2)^{1/2}/(\Gamma^{1/4}R_g)$. For shorter chains, a second order correction term has to be included[34]

$$v^{cc}_{(1)}(r) = -k_BT\frac{\sqrt{5}}{672\pi\rho_{ch}{R_g}^3\Gamma^{1/4}}\left[\frac{945r}{\Gamma^{1/4}R_g}(\cos(Qr) + \sin(Qr)) + 13{Q_{rs}}^3(Qr - 4)\cos(Qr) + \frac{13{Q_{rs}}^4 r}{\Gamma^{1/4}R_g}\sin(Qr)\right]\frac{e^{-Qr}}{Qr} \quad (11)$$

with Q_{rs} being the numerical factor $Q_{rs} = (5^{1/4}(3/2)^{1/2})$ and r in dimensionalized units. These expression define the total direct correlation function and the potential for a liquid of soft spheres of size R_g. It should be stressed that this result is general and does not amount to making the thread limit approximation, but just in assuming $\hat{c}(k)$ to be independent of k for small k, where a coarse-grained description is valid.

The overall schematic of the coarse-graining procedure is represented by Figure 1 First, the appropriate monomer-level description is specified, which in the present case is the PRISM

thread model. Then, the coarse-grained potential can be calculated.

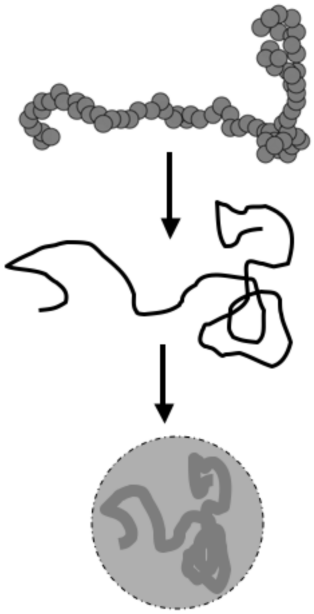

Figure 1. Schematic description of the coarse-graining process. First as an approximate model of the atomistic picture, we represent the actual polymer chain as a Gaussian thread. The parameters from this level of description enter the coarse-graining model, where individual chains are represented as soft colloidal particles, or point particles with a long-range, soft effective interaction.

3. THERMODYNAMICS OF SOFT INTERACTING PARTICLE DESCRIPTION OF A POLYMER MELT

The Hamiltonian of a system of n soft particles labeled with index $i\in\{1,n\}$ is simply the sum of the kinetic and potential energy

$$H = \frac{1}{2m}\sum_{i=1}^{n}({p_{xi}}^2 + {p_{yi}}^2 + {p_{zi}}^2) + \Phi(\mathbf{r}_1, ..., \mathbf{r}_n) \tag{12}$$

where $\Phi(\mathbf{r}_1,...,\mathbf{r}_n)$ is the intermolecular interaction potential. We assume constant temperature, T, and constant volume, V, conditions, consistent with the canonical ensemble in which the atomistic simulations were performed. The partition function for n particles in a volume V is given as

$$Q = \frac{1}{n!h^{3n}}\int ... \int e^{-\beta H}\, d\mathbf{p}_1...d\mathbf{p}_n\, d\mathbf{r}_1...d\mathbf{r}_n \tag{13}$$

where h is Planck's constant and $\beta = 1/k_BT$. Factoring the molecular partition function into an ideal translational term and a perturbation arising from the intermolecular potential formally gives,

$$Q = \frac{1}{n!}(q_{trans}q_{inter})^n \tag{14}$$

with q_{trans} being the classical translational partition function of one atom of a monatomic ideal gas given as

$$q_{trans} = \frac{1}{h^3}\int ... \int \exp\left\{-\frac{({p_x}^2 + {p_y}^2 + {p_z}^2)}{2k_BTm}\right\} dp_x\, dp_y\, dp_z\, dx\, dy\, dz = V/\Lambda^3 \tag{15}$$

where Λ is the thermal de Broglie wavelength. The partition function may be rewritten as

$$Q = \frac{Z_n}{n!\Lambda^{3n}} \tag{16}$$

with Z_n the configurational integral given as

$$Z_n = \int ... \int e^{-\Phi(\mathbf{r}_1,...,\mathbf{r}_n)/k_BT}\, d\mathbf{r}_1...d\mathbf{r}_n \tag{17}$$

such that

$$q_{inter}^n = \frac{Z_n}{V^n} \tag{18}$$

q_{inter} is the contribution to the single particle partition function that is due to the potential. In the soft sphere representation, the potential is pairwise decomposable,

$$\Phi(\mathbf{r}_1, ..., \mathbf{r}_n) = \sum_{1\le i\le j}^{n} v^{cc}(r_{ij}) \tag{19}$$

and the contribution from the interaction potential, q_{inter}, can be written in terms of the mean potential field as

$$q_{inter} = \exp(-\bar{\phi}/2k_BT) = \exp\left(-\frac{2\pi\rho_{ch}}{k_BT}\int_0^\infty v^{cc}(r)g^{cc}(r)r^2\, dr\right) \tag{20}$$

By combining eqs 16, 18, and 20 with the pair distribution functions and effective potentials of our coarse-grained model we will now derive some thermodynamic functions of interest.

In the canonical ensemble the Helmholtz free energy, F, is a natural starting point, given as $F = -k_BT \ln Q$. From eq 16 the free energy of a soft sphere can be expressed in terms of the pair potential as

$$F^{soft} = -nk_BT\ln\left(\frac{Ve}{\Lambda^3 n}\right) + n2\pi\rho_{ch}\int_0^\infty v^{cc}(r)g^{cc}(r)r^2\, dr \tag{21}$$

where the first term is simply the Helmholtz free energy of an ideal gas, F_0, and the second term is a perturbation due to the interaction between point particles through the effective pair potential. For convenience we assume that since the radial distribution function, $g^{cc}(r)$, approaches unity at a much smaller distance than the spatial range of the potential, the integrand is dominated by the contribution arising from the direct correlation function, and $g^{cc}(r)$ is well approximated by the homogeneous limit of $g(r) \cong 1$. This assumption is justified by the soft, long-ranged nature of the pair potential. Noting that the integral of the first order correction term vanishes, eq 21 simplifies to

$$F^{soft} = F_0 + \frac{n\rho_{ch}}{2}\int_0^\infty v_{(0)}^{cc}(r)4\pi r^2\, dr \tag{22}$$

which yields the final result:

dx.doi.org/10.1021/ma301502w | Macromolecules 2012, 45, 8482−8493

$$\frac{F - F_0}{nk_BT} = -\frac{Nc_0\rho}{2} \tag{23}$$

It should be noted that the parameters entering the final expression above come entirely from the monomer-level description, (i.e., there are no fit parameters in our procedure). In principle, eq 23 is general and could be applied to any system once the relevant parameters are chosen. In other words, the exact formulation of c_0 will depend on the monomer-level model which is used, and will be system specific, i.e. it will depend on the chemical architecture of the chain of interest.

Here, we wish to make the connection to the analytical form of the integral equation theory, and thus we use the PRISM thread result for c_0 given by eq 3, to obtain the analytical formula

$$\frac{(F - F_0)_{thread}}{nk_BT} = \frac{\pi\rho\sqrt{N}\sigma^3}{6\sqrt{3}} + \frac{\pi^2\rho^2N\sigma^6}{216} \tag{24}$$

Formally, the total energy of the system of soft spheres is given by

$$\bar{E} = \frac{\int ... \int E e^{-\beta E}\, d\mathbf{r}_1 ... d\mathbf{r}_n}{Q} \tag{25}$$

which under the assumption of a pairwise potential reduces to the well-know expression for the energy of a classical fluid,

$$E^{soft} = \frac{3}{2}nk_BT + n2\pi\rho_{ch}\int_0^\infty v^{cc}(r)g^{cc}(r)r^2\, dr \tag{26}$$

The integral in eq 26 is evaluated under the same approximations used in evaluating eq 21, giving the final result,

$$E^{soft} = \frac{3}{2}nk_BT - nk_BT\frac{Nc_0\rho}{2} \tag{27}$$

where $c_0 < 0$. Again, inserting the PRISM thread expression for c_0 gives the analytical result,

$$\frac{E^{soft}_{thread}}{nk_BT} = \frac{3}{2} + \frac{\pi\rho\sqrt{N}\sigma^3}{6\sqrt{3}} + \frac{\pi^2\rho^2N\sigma^6}{216} \tag{28}$$

The first term in eq 28 is simply the kinetic energy of the n classical point particles, whereas the remaining terms are the ensemble average of the potential energy arising from the interaction potential.

The entropy can be calculated from the identity $E = F + TS$. Interestingly, the contribution to the entropy from the interaction potential cancels out, leaving only the entropy of an ideal gas of point particles,

$$S^{soft} = \frac{3}{2}nk_B + nk_B\ln\left(\frac{Ve}{\Lambda^3 n}\right) \tag{29}$$

Equation 29 may also be obtained directly from the relation $S = k_BT((\partial[\ln Q])/(\partial T))_{n,V} + k_B \ln Q$ using eqs 14−20. The entropy of the underlying real system has additional contributions arising from chain configurations that are not accounted for in the soft sphere model. This is a consequence of coarse graining and will be discussed further below.

Lastly, the pressure is evaluated using the relation, $P = k_BT((\partial[\ln Q])/(\partial V))_{n,T}$, which from eq 16 is simply

$$P = k_BT\left(\frac{\partial[\ln Z_n]}{\partial V}\right)_{n,T} \tag{30}$$

Equation 30 is solved using the standard procedure where the volume limits of the integral in eq 17 are removed by a change of variables. Equation 17 is then substituted into eq 30, differentiated with respect to the volume, and upon returning to the original position vectors gives,

$$\frac{P}{k_BT} = \frac{n}{V} - \frac{1}{k_BTZ_n}\int ... \int e^{-\Phi/k_BT}\frac{\partial\Phi}{\partial V}\, d\mathbf{r}_1 ... d\mathbf{r}_n \tag{31}$$

which is equivalent to

$$P = \rho_{ch}k_BT - \left\langle \frac{\partial\Phi}{\partial V} \right\rangle \tag{32}$$

where $\rho_{ch} = n/V$ is the chain density and

$$\left\langle \frac{\partial\Phi}{\partial V} \right\rangle = \frac{\int ... \int \left(\frac{\partial\Phi}{\partial V}\right) e^{-\Phi/k_BT}\, d\mathbf{r}_1 ... d\mathbf{r}_n}{Z_n} \tag{33}$$

For density-dependent potentials, the volume derivative is often taken to act on the pair potential itself, giving rise to an extra term in the virial equation of state that was pointed out by Ascarelli and Harrison.[48] However, in the case we are considering here, a closed system at fixed volume, the potential is calculated at a fixed given density, and thus the density is a "passive" variable of the system.[49]

Equation 32 recovers the known virial expression for the pressure of a fluid, under the assumption of pairwise additivity,

$$\frac{P}{\rho_{ch}k_BT} = 1 - \frac{2\pi\rho_{ch}}{3k_BT}\int_0^\infty \frac{dv^{cc}(r)}{dr}g^{cc}(r)r^3\, dr \tag{34}$$

Again using the approximation $\beta v^{cc}(r) = -c^{cc}(r)$ and $g^{cc}(r) \approx 1$, eq 34 can be solved from eqs 10 and 12. Noting that the integral of the first order correction term again vanishes, we obtain a simple expression for the equation of state for a fluid of soft spheres,

$$\frac{P}{\rho_{ch}k_BT} = 1 - \frac{Nc_0\rho}{2} \tag{35}$$

In modeling polymers as soft interpenetrating spheres, Louis and co-workers, found that the pressure is described by $\beta P = \rho + 1/2\beta\hat{v}(0)\rho^2$, where $\hat{v}(0)$ is the Fourier transform of the effective potential evaluated at $k = 0$.[50] Their result is consistent with eq 35, where our formalism has the advantage of being fully analytical.

Invoking the thread limit of eq 3 for c_0 gives

$$\frac{P_{thread}}{\rho_{ch}k_BT} = 1 + \frac{\pi\rho\sqrt{N}\sigma^3}{6\sqrt{3}} + \frac{\pi^2\rho^2N\sigma^6}{216} \tag{36}$$

which takes the form of a familiar virial-type expansion of the density, with the second virial coefficient

$$B_2(T) = \frac{\pi\sigma^3}{6\sqrt{3N}} \tag{37}$$

and the third virial coefficient given by

$$B_3(T) = \frac{\pi^2\sigma^6}{216} \tag{38}$$

dx.doi.org/10.1021/ma301502w | Macromolecules 2012, 45, 8482−8493

3.1. Higher Order Corrections to the Soft Sphere Equation of State. Equation 36 is derived under the assumption that the center-of-mass pair potential is $\beta v^{cc}(r) \approx -c^{cc}(r)$. This approximation holds for liquids of long polymer chains, where the center-of-mass of the polymers can easily interpenetrate, $h^{cc}(r) \approx 0$. We now investigate the behavior of the two additional terms in the HNC closure given by eq 6, which are the potential of mean force between center of mass sites, defined as $\beta w^{cc}(r) = -\ln[g^{cc}(r)]$, and the total correlation function, $h^{cc}(r)$. We begin again with the pressure equation, eq 34, which upon introduction of the potential of mean force (pmf) for $v^{cc}(r)$, reduces to

$$\left(\frac{P}{\rho_{ch}k_BT}\right)_{pmf} = 1 + \frac{2}{3}\pi\rho_{ch}\int_0^\infty \frac{dg(r)}{dr} r^3\, dr \tag{39}$$

Equation 39 can be solved analytically using our coarse-grained expression for $g(r)$ from eq 5, with the solution

$$\left(\frac{P_{thread}}{\rho_{ch}k_BT}\right)_{pmf} = 1 + \pi\rho_{ch}R_g{}^2\xi_\rho(1 + \xi_\rho/\xi_c) \tag{40}$$

Introducing the definitions of ξ_ρ and ξ_c, and after some algebra, one obtains

$$\left(\frac{P_{thread}}{\rho_{ch}k_BT}\right)_{pmf} = \frac{3}{2} - \frac{1}{(\sqrt{2} + 2\pi\rho_{ch}R_g{}^3)^2} \tag{41}$$

Comparison of eq 41 with the equation of state calculated above in eq 36, shows that the two are markedly different. Most noticeably, eq 41 scales as $\rho^{-2}N^{-1}$, and in the limit of infinitely long or infinitely dense chains, approaches a constant value of 1.5, which is negligibly small compared to eq 36 which scales as ρ^2N. This supports the validity of the MSA approximation used above for long chains, where $\beta v^{cc}(r) \to -c^{cc}(r)$. In the opposite limit of infinite chain dilution, $\rho_{ch} \to 0$, both eq 36 and eq 41 approach unity, recovering the equation of state for an ideal gas.

Factoring out a $1/R_g{}^2$ and reintroducing the definitions of ξ_c and ξ_ρ, eq 41 can be equivalently written as

$$\left(\frac{P_{thread}}{\rho_{ch}k_BT}\right)_{pmf} = 1 + \frac{1}{R_g{}^2}(\xi_c{}^2 - \xi_\rho{}^2) \tag{42}$$

Equation 42 can be directly compared with the *monomer level* description in the PRISM thread limit, for which $g^{mm}(r)$ is given by eq 2. Upon differentiation of eq 2 with respect to r, and insertion into eq 39, one obtains

$$\left(\frac{P_{thread}}{\rho_{ch}k_BT}\right)_{pmf}^{chain} = 1 + \frac{6}{N\sigma^2}(\xi_c{}^2 - \xi_\rho{}^2)$$

$$= 1 + \frac{1}{R_g{}^2}(\xi_c{}^2 - \xi_\rho{}^2) \tag{43}$$

which is identical with eq 42 obtained in the soft-colloidal representation. Thus, the equation of state derived from the potential of mean force is equivalent in both representations. This is important because a common approach in deriving realistic coarse-grained potentials is to use an iterative procedure, such as the Iterative Boltzmann Inversion method, where the coarse-grained distribution function is optimized against the monomer distribution by iterative calculation of the *potential of mean force* until convergence is reached.[17] Here we have shown how, for dense polymer systems, thermodynamic quantities derived using the potential of mean force in the coarse-grained and monomer representations are formally identical, but also that they are not accurate, as the full pair potential, $v^{cc}(r)$, is needed in the CG simulation.[29]

The third and final contribution in eq 6 to the pressure is again calculated from eq 34, and becomes

$$\left(\frac{P}{\rho_{ch}k_BT}\right)_3 = 1 + \frac{2}{3}\pi\rho_{ch}\int_0^\infty g(r)\frac{dg(r)}{dr} r^3\, dr \tag{44}$$

which can be solved analytically using eq 5, with the solution

$$\left(\frac{P_{thread}}{\rho_{ch}k_BT}\right)_3 = 1 - \pi\rho_{ch}R_g{}^2\xi_\rho(1 + \xi_\rho/\xi_c) + \frac{3087}{1024}\sqrt{\frac{\pi}{6}}\rho_{ch}R_g\,\xi_\rho{}^2\left(1 + \frac{\xi_\rho}{\xi_c}\right)^2 \tag{45}$$

We are now in position to write the total equation of state from the full HNC potential as

$$\left(\frac{P}{\rho_{ch}k_BT}\right)_{tot} = \left(\frac{P}{\rho_{ch}k_BT}\right)_{MSA} + \left(\frac{P}{\rho_{ch}k_BT}\right)_{pmf} + \left(\frac{P}{\rho_{ch}k_BT}\right)_3 \tag{46}$$

Combining eq 35, 40, and 44 gives,

$$\left(\frac{P_{thread}}{\rho_{ch}k_BT}\right)_{tot} = 1 + \frac{\pi\rho\sqrt{N}\sigma^3}{6\sqrt{3}} + \frac{\pi^2\rho^2N\sigma^6}{216} + \frac{3087}{1024}\sqrt{\frac{\pi}{6}}\rho_{ch}\,R_g\xi_\rho{}^2\left(1 + \frac{\xi_\rho}{\xi_c}\right)^2 \tag{47}$$

Not surprisingly, the addition of eq 40 and eq 45 results in a cancellation of the potential of mean force term.

The additional term in eq 47 resulting from the inclusion of the full HNC potential, scales as $\rho^{-1}N^{-1/2}$. Thus, for large N the MSA approximation for which $\beta v^{cc}(r) \approx -c^{cc}(r)$ is increasingly valid and $P^{tot} \approx P^{MSA}$ as given by eq 36.

Figure 2 shows the contributions to the total equation of state from each of the terms in eq 46 for a representative case where the monomer density is $\rho = 0.0334$ sites/Å^3 and effective segment length of $\sigma = 4.036$ Å. It shows that the equation of state is dominated by the contribution from the MSA approximation term, and the additional contributions rapidly approach their asymptotic value.

3.2. The Compressibility Route. An alternative approach to calculate the thermodynamic properties of fluids is to use the compressibility route, which is derived in the grand canonical ensemble, where particle number fluctuations may be readily obtained, and is found to depend solely on density fluctuations. More specifically, the reduced equation of state obtained from the compressibility route is determined by thermodynamic integration of the isothermal compressibility, κ_T, which is related to $\hat{S}^{cc}(k \to 0)$, and reads[44]

$$\frac{P}{k_BT} = \int_0^{\rho_{ch}} d\rho\, [\hat{S}^{cc}(0, \rho)]^{-1}] \tag{48}$$

Using the form of the reciprocal structure factor given above by eq 9, recalling that $\Gamma = -Nc_0\rho$, the integral in eq 48 can be

dx.doi.org/10.1021/ma301502w | Macromolecules 2012, 45, 8482−8493

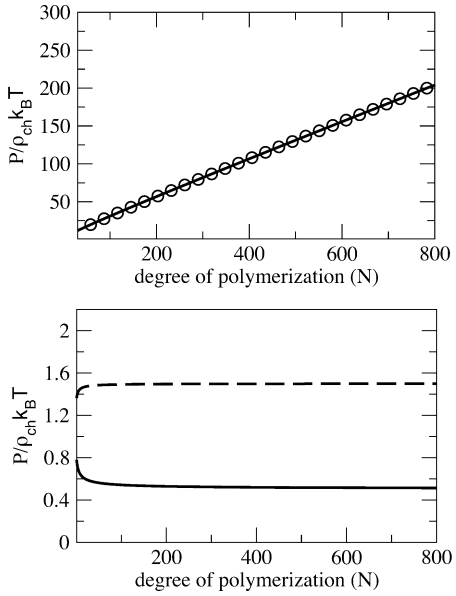

Figure 2. Top: The equation of state obtained from the MSA approximation, eq 36 is shown (open circles) in comparison with the full equation of state using the HNC potential, eq 47 (solid line) for the PRISM thread model. The two lines superimpose and are nearly indistinguishable, both scaling linearly with N for large N. Bottom: For comparison is show the contributions to the equation of state from eqs 40 and 45, both of which quickly approach their asymptotic value with N^{-1} scaling for the potential of mean force term (dashed line) and with $N^{-1/2}$ scaling for the third term (solid line).

solved to obtain the compressibility equation of state. A general expression for the density dependence of c_0 is not available. As a first estimate, we could ignore any explicitly density dependence of c_0 (i.e., $c_0(\rho) = c_0$), giving

$$\left(\frac{P}{\rho_{ch}k_BT}\right)_c = -\frac{Nc_0\rho}{2} \tag{49}$$

which is identical with eq 35, showing that the compressibility route and the virial route in this case are equivalent. Also, as shown below, this is equivalent with the monomer-level prediction.

Alternatively, one could introduce a density dependence to c_0, for example with the thread limit (eq 3), and obtain a slightly different expression. Insertion of eq 3 into $[\hat{S}^{cc}(0)]^{-1} = -Nc_0\rho$, and subsequent integration yields

$$\left(\frac{P_{thread}}{\rho_{ch}k_BT}\right)_c = \frac{\pi\rho\sqrt{N}\sigma^3}{6\sqrt{3}} + \frac{2}{3}\frac{\pi^2\rho^2N\sigma^6}{216} \tag{50}$$

Comparison of eq 50 with eq 36 shows that, although not exactly identical, the difference between the two routes in this case is only in the numerical prefactor of the third virial coefficient and not in the overall scaling, which is consistent with the use of the PY closure used to derive the thread limit.

As a test for self-consistency in our theoretical expressions, we can compare the above expression, which was derived from eq 9, with that obtained using the analytical expression of the total correlation function, $h^{cc}(k)$, derived from Yatsenko, et al.,[6] which can be obtained from integration of eq 5, and is given as

$$\hat{h}^{cc}_{thread}(k=0) = -\left[1 - \left(\frac{\xi_\rho}{\xi_c}\right)^2\right]/\rho_{ch} \tag{51}$$

Equation 51 provides an expression for the isothermal compressibility, κ_T, related to the structure factor as $\rho_{ch}\kappa_T/\beta = \hat{S}(0) = 1 + \rho_{ch}\hat{h}(0) = (\xi_\rho/\xi_c)^2$. By evaluation of eq 48 using our definition for $\hat{h}^{cc}(0)$, one finds

$$\left(\frac{P_{thread}}{\rho_{ch}k_BT}\right)_c = 1 + \sqrt{2}\,\pi\rho_{ch}{R_g}^3 + \frac{2}{3}\pi^2{\rho_{ch}}^2{R_g}^6$$

$$=1 + \frac{\pi\rho\sqrt{N}\sigma^3}{6\sqrt{3}} + \frac{2}{3}\frac{\pi^2\rho^2N\sigma^6}{216} \tag{52}$$

where the second expression is obtained using the definition of the effective segment length, $R_g = (N/6)^{1/2}\sigma$, and recovers exactly the form of eq 50, indicating that the approximate forms for $c^{cc}(r)$ and $[S^{cc}(k)]^{-1}$ are consistent in recovering the compressibility of the coarse-grained system.

Using our coarse-graining procedure for polymer melts, we have now obtained simple, analytical expressions for the reduced equation of state from both the virial route and the compressibility route under different assumptions. Comparison of the reduced equation of state from these different methods show reasonable agreement indicating the consistency of our renormalization procedure and that our analytical form of the direct correlation function and effective pair potential are well determined. We now turn to a more detailed discussion about the equivalence of our expressions with the monomer level description.

4. EQUIVALENCE WITH MONOMER LEVEL DESCRIPTION

At this point, we turn to a monomer-level chain description in order to see which of the relationships derived above hold and what information may be lost in coarse-graining. Notationally, the position vector, $\mathbf{r}_I^\alpha$ refers to the position of site α on chain i, whereas $\mathbf{r}_{ij}^{\alpha,\gamma}$ is the distance between site α on chain i and site γ on chain j. Extending the above approach to chain molecules requires the inclusion of intramolecular energy terms such that eq 14 becomes

$$Q = \frac{1}{(nN)!}(q_{trans}q_{inter}q_{intra})^{nN} \tag{53}$$

where q_{trans} is the translational partition function, q_{inter} is the intermolecular contribution to the partition function and q_{intra} is the intramolecular contribution which will depend on the specific model being used, but will generally include vibrational, angular, torsional, and nonbonded terms. Integration over the $3nN$ independent Cartesian momenta gives,

$$Q = \frac{Z_{nN}}{(nN)!\Lambda^{3nN}} \tag{54}$$

where Z_{nN} is the configurational integral given as

$$Z_{nN} = \int \cdots \int e^{-(\Phi_{inter}+\Phi_{intra})/k_BT}\, d\mathbf{r}_1^1 \ldots d\mathbf{r}_n^N \tag{55}$$

where we have separated the potential energy into intermolecular and intramolecular terms.

The energy of the liquid of chains is,

dx.doi.org/10.1021/ma301502w | Macromolecules 2012, 45, 8482−8493

$$E^{chain} = \frac{3}{2}nNk_BT + \langle \Phi_{inter} \rangle + \langle \Phi_{intra} \rangle \tag{56}$$

where $\langle \Phi_{inter} \rangle$ is the average intermolecular contribution to the energy and $\langle \Phi_{intra} \rangle$ is the average intramolecular contribution. The first term is given by

$$\left\langle \Phi_{inter} \right\rangle = \frac{\int \dots \int \Phi_{inter} e^{-(\Phi_{inter}+\Phi_{intra})/k_BT} \, d\mathbf{r}_1^1 \dots d\mathbf{r}_n^N}{Z_{nN}} \tag{57}$$

The true monomer-level description may not be pairwise additive and higher order correlations will enter between monomers. However, for the sake of simplicity, we assume pairwise additivity, and thus

$$\Phi_{inter} = \sum_{i>j=1}^{n} \sum_{\alpha,\gamma=1}^{N} v_{\alpha\gamma}(r_{ij}^{(\alpha\gamma)}) \tag{58}$$

where $v_{\alpha\gamma}(r_{ij}^{(\alpha\gamma)})$ is the intermolecular pair potential between site α on molecule i and site γ on molecule j.

The intramolecular contribution is given as

$$\langle \Phi_{intra} \rangle = \frac{\int \dots \int \Phi_{intra} e^{-(\Phi_{inter}+\Phi_{intra})/k_BT} \, d\mathbf{r}_1^1 \dots d\mathbf{r}_n^N}{Z_{nN}} \tag{59}$$

The intramolecular potential will depend on the specific monomer chain model, and could include excluded volume, bond, angular, and torsional contributions. In this work, we focus only on the athermal thread limit, which is a highly idealized description for a polymer, for which Φ_{intra} will only have an excluded volume contribution equivalent to the intermolecular potential. An extension to more realistic bead−spring models for polymer chains is straightforward and will be presented in a forthcoming paper.

The intramolecular excluded volume potential is written as a sum of pairwise additive terms,

$$\Phi_{intra} = \sum_{i=1}^{n} \sum_{\alpha,\gamma=1}^{N} v_{\alpha,\gamma}(r_{ii}^{(\alpha\gamma)}) \tag{60}$$

so that the total energy can be written as

$$E = \frac{3}{2}nNk_BT + \frac{nN\rho}{2} \int_0^\infty 4\pi g(r) v(r) r^2 \, dr \tag{61}$$

where $g(r)$ is the total radial distribution function of monomers.

In the athermal PRISM thread limit, the potential is taken to be a purely repulsive hard core interaction, and the Percus−Yevick (PY) closure is adopted

$$c(r) = (1 - e^{v(r)/k_BT}) g(r) \tag{62}$$

which can be approximated by expanding the exponential to first order, such that

$$-k_BTc(r) \approx v(r)g(r) \tag{63}$$

Substitution into eq 61 immediately gives

$$\frac{E}{nk_BT} = \frac{3}{2}N - \frac{N\rho c_0}{2} \tag{64}$$

which is identical with the result obtained from the coarse-grained potential except that the kinetic energy is increased by a factor of N.

The pressure equation for chain molecules has been rigorously discussed by Honnell, Hall, and Dickman.[51] Contributions from the intramolecular potential will depend on the particulars of the monomer-level description used. In the thread model, the only intramolecular contribution is the hard core excluded volume interaction, and the pressure is given by

$$\left(\frac{P}{\rho_{ch}k_BT}\right)_{chain} = 1 - \frac{2\pi\rho_{ch}}{3k_BT} \sum_{\alpha,\gamma=1}^{N} \int_0^\infty g_{\alpha\gamma}(r) \frac{dv_{\alpha\gamma}(r)}{dr} r^3 \, dr + R_3 \tag{65}$$

where R_3 can be written in terms of a three-body distribution function, shown by Schweizer and Curro to be equivalent to[52]

$$R_3 = -\frac{1}{3k_BT} \frac{\rho_{ch}}{N-1} \sum_{\alpha,\gamma,\lambda=1}^{N} \int d\mathbf{r} \int d\mathbf{r}' \, \hat{\mathbf{r}}\cdot\mathbf{r}' \frac{dv^{mm}(r)}{dr} g_{\alpha\lambda,\gamma}^{(3)}(\mathbf{r}, \mathbf{r}') \tag{66}$$

where $g_{\alpha\lambda,\gamma}^{(3)}(\mathbf{r},\mathbf{r}')$ is the joint probability distribution function for site α on chain i and site γ on chain j to be separated by distance $\mathbf{r}$ *and* for site α on chain i and site λ on the *same* chain i to be separated by distance $\mathbf{r}'$. Schweizer and Curro have shown that the quantity R_3 scales as $\rho^{-1}N^{-1/2}$ and is therefore negligible for infinitely long or infinitely dense chains. Here we focus on the first term in eq 65. From eq 63, along with the thread limit definition of $c(r)$, the derivative of the potential becomes

$$\frac{dv_{\alpha\gamma}(r)}{dr} = -\frac{3v_{\alpha\gamma}(r)}{r} \tag{67}$$

Insertion of eq 67 into eq 65 gives

$$\left(\frac{P}{\rho_{ch}k_BT}\right)_{chain} = 1 + \frac{\rho_{ch}}{2k_BT} \sum_{\alpha,\gamma=1}^{N} \int_0^\infty 4\pi g_{\alpha\gamma}(r) v_{\alpha\gamma}(r) r^2 \, dr \tag{68}$$

Insertion of eq 63 along with the PRISM thread $c(r)$ in the site averaged limit gives the desired result

$$\left(\frac{P}{\rho_{ch}k_BT}\right)_{chain} = 1 - \frac{\rho N c_0}{2} \tag{69}$$

which is precisely equivalent with the result in the coarse-grained description. This is important as it demonstrates that thermodynamic information is not lost during the coarse-graining procedure, as the bulk properties of a fluid should not depend on the frame of reference used.

4.1. The Compressibility Route. The equivalence between the two levels of description is readily seen in the compressibility route. This is because the formalism inherent in our coarse-graining method is based on determining the center of mass total correlation function, $h^{cc}(r)$, by utilizing the relationship expressed through eq 4. In the $k = 0$ limit, both of the intramolecular form factors reduce to $\hat{\omega}(0) = N$, and it is immediately seen that $\hat{h}^{cc}(0) = \hat{h}^{mm}(0)$.

In the monomer frame of reference, the exact recovery of eq 52 is arrived at by using the PRISM thread limit for $h^{mm}(k)$,

$$h_{thread}^{mm}(k) = 4\pi\xi_\rho' \left[\frac{\xi_\rho^{\,2}}{1 + k^2\xi_\rho^{\,2}} - \frac{\xi_c^{\,2}}{1 + k^2\xi_c^{\,2}} \right] \tag{70}$$

with the quantity, $\xi_\rho' = 1/(2\pi\rho_{ch}R_g^{\,2})$. Taking the $k = 0$ limit of eq 70, one recovers eq 51 in the monomer frame of reference.

dx.doi.org/10.1021/ma301502w | Macromolecules 2012, 45, 8482−8493

At the monomer level, $\hat{S}^{mm}(0) = \hat{\omega}(0) + \rho h^{mm}(0) = N(\xi_\rho/\xi_c)^2$, and the integration is carried out over the monomer density of sites,

$$\left(\frac{P}{k_B T}\right)_{chain} = \int_0^\rho d\rho[\hat{S}^{mm}(0,\rho)]^{-1}]$$

$$= \rho_{ch} + \sqrt{2}\pi\rho_{ch}{}^2 R_g{}^3 + \frac{2}{3}\pi^2\rho_{ch}{}^3 R_g{}^6 \quad (71)$$

which is equivalent to eq 52 upon division by ρ_{ch}.

The free energy can be readily computed via the standard thermodynamic integration of the pressure,[53]

$$\frac{F}{nk_B T} = \int_0^\rho \frac{d\rho'}{\rho'}\frac{NP}{\rho' k_B T} \quad (72)$$

Substitution of eq 71 into eq 72 and subsequent integration gives

$$\frac{(F - F_0)_{thread}}{nk_B T} = \frac{\pi\rho\sqrt{N}\sigma^3}{6\sqrt{3}} + \frac{1}{3}\frac{\pi^2\rho^2 N\sigma^6}{216} \quad (73)$$

where we have used $\sigma = (6/N)^{1/2}R_g$. Both eq 71 and eq 73 have been derived elsewhere by Chatterjee and Schweizer for a homopolymer fluid.[54] Comparison of eq 73 with our result for the coarse grained model given by eq 24 show that the two are nearly equivalent with a slightly different prefactor in the final term which comes from the difference between the compressibility and virial route expressions.

5. COMPARISON OF ANALYTICAL EXPRESSIONS WITH MOLECULAR DYNAMICS SIMULATIONS OF SOFT SPHERES

Our coarse-graining procedure enables one to perform molecular dynamics simulations of large ensembles of polymers, each represented by a single center of mass site interacting with other sites through an effective potential. These simulations are designated as mesoscale (MS) simulations as they provide information about intermediate time and length scales. Having derived various analytical formulas for thermodynamic properties of interest, our goal in this section is to demonstrate the consistency between these theoretical expressions and mesoscale simulations.

Any coarse-graining scheme is only as accurate as the more detailed molecular model from which it is derived. Since we have shown that our expressions recover the known PRISM result when the PRISM thread expression for c_0 is used, this can be seen as a self-consistency check between thermodynamic quantities calculated directly from MS simulation and from theory.

We perform simulations of particles interacting via the full HNC potential of eq 4 implemented numerically, along with simulations using the approximate analytical expression of eq 10. The procedure to obtain the pair potential is as follows: First, eq 4 is used to obtain $h^{cc}(k)$. For the monomer intramolecular distribution we use the Debye formula whereas for the distribution of monomers about the center of mass we employ a Gaussian form.[6] For $h^{mm}(k)$ we use the Ornstein–Zernike equation, given by eq 1, with $c^{mm}(k)$ approximated as c_0 given by the thread limit result of eq 3 . From $h^{cc}(k)$, we obtain $c^{cc}(k)$ from eq 7. Numerical Fourier Transform of both $h^{cc}(k)$ and $c^{cc}(k)$ yields the desired potential, $v^{cc}(r)$ through the HNC closure given by eq 6.

The only parameters entering the model are σ, ρ, T, and N. To test our expressions we perform mesoscale simulations for two different sets of chain lengths with differing monomer densities. The first set with $N = 100$, $T = 450$ K, and an effective segment length of $\sigma = 4.08$Å. The second set with $N = 500$, $T = 450$ K, and $\sigma = 4.415$ Å.

Mesoscale simulations of point particles interacting through the soft effective potential have been described elsewhere.[36,42] Briefly, the simulations are performed using the LAMMPS code[55] in parallel using the SDSC Trestles cluster available through XSEDE. Simulations were run in the *NVT* ensemble, using a Nose-Hoover thermostat with periodic boundary conditions. The pressure in the mesoscale simulation is calculated using the standard virial relation

$$P = \frac{nk_B T}{V} + \frac{\sum_i^n r_i \cdot f_i}{3V} \quad (74)$$

The average total, kinetic, and potential energy was also calculated from the simulation.

The number of particles included in a simulation is chosen to maintain the density of chains in the atomistic description; hence $\rho_{ch} = \rho/N$. Since the volume must increase with the range of the potential, it is convenient to cut the potential at some distance, r_{cut}, after which the particles do not interact. However, cutting the potential introduces effects on the calculated thermodynamic quantities. The soft potential has the general form of a damped oscillating function. For the $N = 100$ set of simulations we chose to cut the potential where the derivative passes through zero to avoid any discontinuities in the force. The top panel of Figure 3 shows the potential for a representative density ($\rho = 0.78$ g/mL). The potential was cut where the derivative (shown on the right) passes through zero,

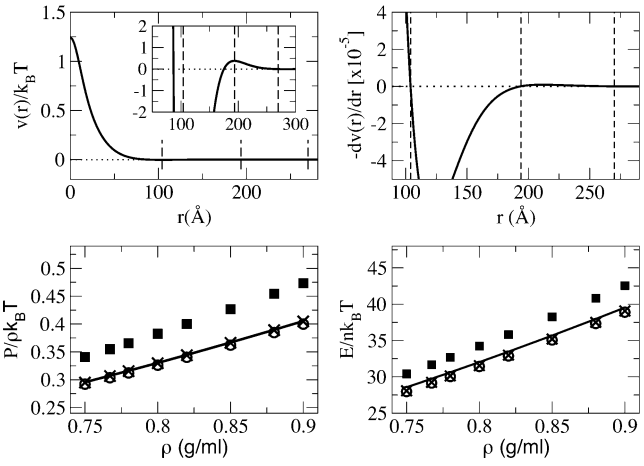

Figure 3. Soft potential (top left) calculated for the representative case for PE with $N = 100$ and $\rho = 0.78$ g/mL. The dashed lines indicate the distances at which the potential was cut, which occur where the force crosses zero (top right). The inset highlights the region where the potential is cut. The bottom panels show the pressure (bottom left) and potential energy (bottom right) calculated directly from mesoscale simulations of point particles using the numerical HNC potential cut after the first repulsive peak (squares), the first repulsive plus first attractive well (open circles) and after the first repulsive, first attractive, and second repulsive peak (crosses). For comparison, simulations using the analytic approximation were also run (open circles) and the points superimpose. Comparison is made with our analytical prediction given by eq 36 and eq 28 (solid line) for different densities.

dx.doi.org/10.1021/ma301502w | Macromolecules 2012, 45, 8482–8493

which were for this density at r_{cut} = 104, 194, and 270 Å. The bottom panels of Figure 3 show the calculated thermodynamic quantities as compared to our analytical expressions for the thread model. Cutting the potential after just the first repulsive part leads to an overestimate of the pressure and energy, whereas including the small attractive tail nearly completely corrects for this. The agreement is quantitative when the second repulsive barrier is included. Comparison between the numerical HNC potential and the analytical approximation of eq 10 are indistinguishable on the plot with a difference of less than 2%.

Figures 4 and 5 show a comparison between the pressure and potential energies (respectively) as predicted from our

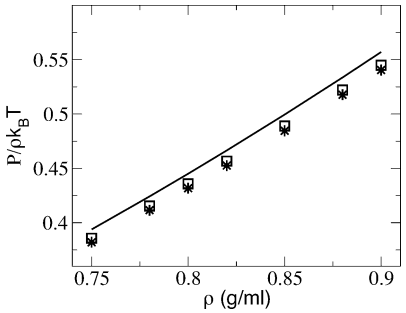

Figure 4. Comparison between the pressure calculated directly from mesoscale simulations of point particles using the numerical HNC potential(open squares) with mesoscale simulations performed using the analytical approximation (stars). For comparison, the analytical prediction for the pressure given by eq 36 is shown (line) for different densities of PE with N = 500.

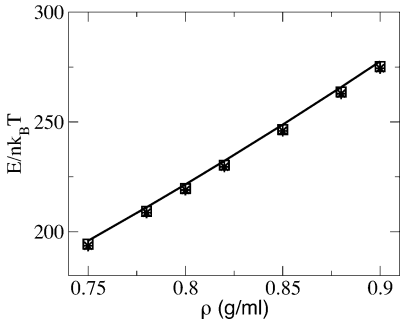

Figure 5. Comparison between the potential energy calculated directly from the average of the mesoscale simulation using the HNC (open squares) and the approximate analytical potential (stars). Comparison is also made with the analytical prediction given by eq 28 (line) for PE with N = 500.

analytical formula against those calculated directly from MD simulations using the numerical HNC potential as well as the analytical approximation. For the set of simulations with N = 500 we show only the results where the potential was cut after the first repulsive plus first attractive well in the force. Results show quantitative agreement between theory at the monomer and CG levels of description, as well as consistency with data from mesoscale simulations, indicating that the thermodynamics for our soft sphere model are well understood.

6. CONCLUSION

In this paper, we have presented a detailed study of the structural and thermodynamic properties of a coarse-grained model where polymer melts are represented as liquids of soft interacting spheres. The CG procedure builds on the first principles Ornstein−Zernike equation, which formally relates the pair distribution function for the CG description with the atomistic pair distribution functions. From the pair distribution functions the thermodynamics of the atomistic and coarse-grained descriptions are formally calculated and proven to be fully consistent. An analytical solution for the soft-colloidal equation of state is made possible by utilizing an approximate formulation of the polymer center of mass direct correlation function and the related effective potential.

The paper also presents a direct comparison to mesoscale simulations that use the derived effective potential as an input. Results are presented for both a general framework where the underlying monomer-level description is not specified, and, as an illustrative example, for the PRISM thread model. Atomistic and CG descriptions, as well as mesoscale simulations are shown to be fully consistent, demonstrating that the described CG procedure formally maintains both structural and thermodynamic properties of the system under study during coarse-graining.

Because thermodynamic consistency is formally attained, it is possible to identify key features in the formalism that are important for the consistency of the thermodynamic procedure, including characteristic scaling exponents. Not only the effective potential between two CG units is solved analytically, but also a formal solution of the mean-force potential is presented, which show how consistency between atomistic and coarse-grained descriptions is maintained also for quantities calculated using the mean-force potential. However, properties derived from the mean-force potential are formally different from the ones calculated with the correct potential, suggesting that in self-consistent procedures of optimization the potential of mean force might not be the optimal choice as the starting potential.

AUTHOR INFORMATION

Corresponding Author

*E-mail: mguenza@uoregon.edu.

Notes

The authors declare no competing financial interest.

ACKNOWLEDGMENTS

We acknowledge support from the National Science Foundation through grant DMR-0804145. Computational resources were provided by Trestles through the XSEDE project supported by NSF. This research was supported in part by the National Science Foundation under Grant No. PHY11-25915.

REFERENCES

(1) *Monte Carlo and Molecular Dynamics Simulations in Polymer Science*; Binder, K., Ed.; Oxford University Press: New York, 1995.

(2) Baschnagel, J.; Binder, K.; Doruker, P.; Gusev, A. A.; Hahn, O.; Kremer, K.; Mattice, W. L.; Müller-Plathe, F.; Murat, M.; Paul, W.; Santos, S.; Suter, U. W.; V. Tries, V. *Adv. Polym. Sci.* **2000**, *200*, 41.

(3) Theodorou, D. N. Equilibration and Coarse-Graining Methods for Polymers. *Lect. Notes Phys.* **2006**, *704*, 419.

(4) Hou, J.-X.; Svaneborg, C.; Everaers, R.; Grest, G. S. *Phys. Rev. Lett.* **2010**, *105*, 068301.

(5) Auhl, R.; Everaers, R.; Grest, G. S.; Kremer, K.; Plimpton, S. J. *J. Chem. Phys.* **2003**, *119*, 12718.

(6) Yatsenko, G.; Sambriski, E. J.; Nemirovskaya, M. A.; Guenza, M. *Phys. Rev. Lett.* **2004**, *93*, 257803.

(7) Yatsenko, G.; Sambriski, E. J.; Guenza, M. G. *J. Chem. Phys.* **2005**, *122*, 054907.
(8) Sambriski, E. J.; Yatsenko, G.; Nemirovskaya, M. A.; Guenza, M. G. *J. Chem. Phys.* **2006**, *125*, 234902.
(9) Sambriski, E. J.; Guenza, M. G. *Phys. Rev. E.* **2007**, *76*, 051801.
(10) Clark, A. J.; Guenza, M. G. *J. Chem. Phys.* **2010**, *132*, 044902.
(11) Neri, M.; Anselmi, C.; Cascella, M.; Maritan, A.; Carloni, P. *Phys. Rev. Lett.* **2005**, *95*, 218102.
(12) Guenza, M. G. *J. Phys.: Condens. Matter* **2008**, *20*, 033101.
(13) Chen, l.-j.; Quian, H.-J.; Lu, Z.-Y.; Li, Z.-S.; Sun, C. C. *J. Phys. Chem. B* **2006**, *110*, 24093.
(14) Harmandaris, V. A.; Reith, D.; van der Vegt, N. F. A.; Kremer, K. *Macromol. Chem. Phys.* **2007**, *208*, 2109.
(15) Praprotnik, M.; Site, L. D.; Kremer, K. *Annu. Rev. Phys. Chem.* **2008**, *59*, 545.
(16) Sun, Q.; Ghosh, J.; Faller, R. *State point dependence and transferability of potentials in systematic structural coarse graining*. In *Coarse-Graining of Condensed Phase and Biomolecular Systems*; Voth, G.; Ed.; CRC Press: Boca Raton, FL, 2008.
(17) Reith, D.; Pütz, M.; Müller-Plathe, F. *J. Comput. Chem.* **2003**, *24*, 1624.
(18) Lyubartsev, A. P.; Laaksonen, A. *Phys Rev. E.* **1995**, *52*, 3730.
(19) Izvekov, S.; Voth, G. A. *J. Chem. Phys.* **2005**, *123*, 134105.
(20) Izvekov, S.; Voth, G. A. *J. Phys. Chem. B* **2005**, *109*, 2469.
(21) Praprotnik, M.; Junghans, C.; Site, L. D.; Kremer, K. *Comput. Phys. Commun.* **2008**, *179*, 51.
(22) Nielsen, S. O.; Lopez, C. F.; Srinivas, G.; Klein, M. L. *J. Chem. Phys.* **2003**, *119*, 7043.
(23) Knotts, T. A., IV; Rathore, N.; Schwartz, D. C.; de Pablo, J. J. *J. Chem. Phys.* **2007**, *126*, 084901.
(24) de Pablo, J. J. *Annu. Rev. Phys. Chem.* **2011**, *62*, 555.
(25) Louis, A. A. *J. Phys.: Condens. Matter* **2002**, *14*, 9187.
(26) Fukunaga, H.; Takimoto, J.; Doi, M. *J. Chem. Phys.* **2002**, *116*, 8183.
(27) Carbone, P.; Varzaneh, H. A. K.; Chen, X.; Müller-Plathe, F. *J. Chem. Phys.* **2008**, *128*, 064904.
(28) Henderson, R. L. *Phys. Lett. A* **1974**, *49*, 197.
(29) McQuarrie, D. A. *Statistical Mechanics*: University Science: Sausalito, CA, 2000.
(30) Jain, S.; Garde, S.; Kumar, S. K. *Ind. Eng. Chem. Res.* **2006**, *45*, 5614.
(31) Johnson, M. E.; Head-Gordon, T.; Louis, A. A. *J. Chem. Phys.* **2007**, *126*, 144509.
(32) Müller-Plathe, F. *Chem. Phys. Chem.* **2002**, *3*, 754.
(33) Clark, A. J.; McCarty, J.; Lyubimov, I. Y.; Guenza, M. G. *Phys. Rev. Lett.* (in print).
(34) Clark, A. J.; Guenza, M. G. Manuscript in preparation.
(35) Ashbaugh, H. S.; Patel, H. A.; Kumar, S. K.; Garde, S. *J. Chem. Phys.* **2005**, *122*, 104908.
(36) Lyubimov, I. Y.; McCarty, J.; Clark, A.; Guenza, M. G. *J. Chem. Phys.* **2010**, *132*, 224903.
(37) Schweizer, K. S.; Curro, J. G. *Adv. Chem. Phys.* **1997**, *98*, 1.
(38) de Gennes, P.-G. *Scaling Concepts in Polymer Physics*;Cornell University Press: Ithaca, NY, 1979.
(39) Schweizer, K. S.; Curro, J. G. *Adv. Chem. Phys.* **1997**, *98*, 1; *Adv. Polym. Sci.* **1994**, *116*, 319.
(40) Schweizer, K. S.; Curro, J. G. *Macromolecules* **1998**, *21* (3070), 3082; *J. Chem. Phys.* **1990**, *149*, 105.
(41) Krakoviack, V.; Hansen, J.-P.; Louis, A. A. *Europhys. Lett.* **2002**, *58*, 53.
(42) McCarty, J.; Lyubimov, I. Y.; Guenza, M. G. *J. Phys. Chem. B* **2009**, *113*, 11876.
(43) McCarty, J.; Guenza, M. G. *J. Chem. Phys.* **2010**, *133*, 094904.
(44) Hansen, J.-P.; McDonald, I. R. *Theory of Simple Liquids*; Academic Press: London, 1991.
(45) Rosenfeld, Y.; Ashcrof, N. W. *Phys. Rev. A* **1979**, *20*, 2162.
(46) Tang, Y.; Lu, B. C.-Y. *AIChE J.* **1997**, *43*, 2215.
(47) Schweizer, K. S.; Yethiraj, A. *J. Chem. Phys.* **1993**, *98*, 9053. Yethiraj, A.; Schweizer, K. S. *ibid* **1993**, *98*, 9080.
(48) Ascarelli, P.; Harrison, R. J. *Phys. Rev. Lett.* **1969**, *22*, 385.
(49) Stillinger, F. H.; Sakai, H.; Torquato, S. *J. Chem. Phys.* **2002**, *117*, 288.
(50) Louis, A. A.; Bolhuis, P. G.; Hansen, J. P.; Meijer, E. J. *Phys. Rev. Lett.* **2000**, *85*, 2522.
(51) Honnell, K. G.; Hall, C. K.; Dickman, R. *J. Chem. Phys.* **1987**, *87*, 664.
(52) Schweizer, K. S.; Curro, J. G. *J. Chem. Phys.* **1988**, *89*, 3342. Schweizer, K. S.; Curro, J. G. *J. Chem. Phys.* **1988**, *89*, 3350.
(53) Oyerokun, F. T.; Schweizer, K. S. *J. Phys. Chem. B* **2005**, *109*, 6595.
(54) Chatterjee, A. P.; Schweizer, K. S. *J. Chem. Phys.* **1998**, *108*, 3813.
(55) Plimpton, S. *J. Comput. Phys.* **1995**, *117*, 1.